



ELSEVIER

Contents lists available at ScienceDirect

Journal of Magnetism and Magnetic Materials

journal homepage: www.elsevier.com/locate/jmmm

Research articles

Ferromagnetic resonance in iron tubes deposited on a copper grid

S.V. Stolyar^{a,b,c}, R.N. Yaroslavtsev^{a,b,c,*}, L.A. Chekanova^b, M.V. Rautskii^b, O.A. Bayukov^b, E.V. Cheremiskina^c, I.V. Nemtsev^b, M.N. Volochaev^b, R.S. Iskhakov^b^a Krasnoyarsk Scientific Center, Federal Research Center KSC SB RAS Krasnoyarsk, Russia^b Kirensky Institute of Physics, Federal Research Center KSC SB RAS, Krasnoyarsk, Russia^c Siberian Federal University, Krasnoyarsk, Russia

ARTICLE INFO

Keywords:

Magnetic tubes

Ferromagnetic resonance

ABSTRACT

In the work, a composite material, which is an iron coating on a copper microgrid with a mesh size of 50 μm , is investigated. Iron coatings were synthesized by electroless deposition using arabinogalactan as a reducing agent. Samples were investigated using transmission electron microscopy, Mossbauer spectroscopy and ferromagnetic resonance methods. Magnetic anisotropy in the grid plane was studied by measuring the FMR spectra. The results of the study are discussed by modeling the composite as a wireframe system of magnetic tubes.

1. Introduction

Due to small size and unique properties, nanowires and nanotubes are attractive for many applications, such as data storage [1], catalysis [2], sensing [3,4], and biomedicine [5–7]. The properties of arrays of microwires can be used in devices for processing radio frequency signals. Metal grid consisting of electrically conductive wires can be used as microwave absorbers and to protect against electromagnetic interference [8]. Such structures called frequency-selective surfaces for electromagnetic waves. They can be used in filters and other devices [9,10]. The absorption of electromagnetic waves can be due to ferromagnetic resonance. The resonant frequency is highly dependent on the material, but also on the shape of the magnet. Unlike films, resonance in rod-shaped objects and, consequently, microwave absorption also occurs without the application of an external magnetic field. The operating frequency range can be selected by varying the material and packing density of the wires. The frequency can be further tuned over a wide range by applying a magnetic field. Ferromagnetic resonance in nanowires has been studied quite well, but there are a limited number of studies on ferromagnetic resonance in nanotubes [11–13].

In this work, an electroless deposition method was used to produce an iron coating [14,15]. The process of chemical precipitation is autocatalytic. The reduction of metal ions in solution is carried out due to the oxidation of the reducing agent. As a reducing agent, compounds such as hypophosphite, borohydride, hydrazine are commonly used. A new approach to metal recovery is currently being developed, using extracts of natural plant products. Such extracts are generally non-toxic, and function as a dispersing and coating agent, minimizing oxidation

and agglomeration processes. As a reducing agent, we used arabinogalactan [16,17], isolated from larch, to obtain an iron coating on a copper grid. The molecule of arabinogalactan consists of galactose and arabinose units. The corresponding monosaccharides have an aldehyde group that has reducing properties.

2. Material and methods

Iron coatings were synthesized by electroless deposition using arabinogalactan as a reducing agent on a base, which is a grid of copper wires with a mesh size of 50 μm and coated with palladium. Deposition was carried out from an aqueous solution of the following composition: iron sulfate – 30 g/l, sodium citrate – 50 g/l, EDTA-Na₂ – 20 g/l, arabinogalactan – 10 g/l, NaOH to reach 11 pH. The temperature of the solution was maintained with a thermostat at 85 °C. The iron reduction reaction is accompanied by the reaction of reducing arabinogalactan to carbon, and therefore the synthesized coating has graphite inclusions. Since the copper fibers that make up the grid have the shape of a cylinder with an outer diameter of 10 μm , the result is a regular grid of micro-tubes with an inner diameter equal to the diameter of the copper fibers, with the axis of the micro-tubes lying in the same plane.

Electron microscopic studies were carried on a Hitachi HT7700 transmission electron microscope (accelerating voltage 100 kV) and a FE SEM Hitachi S-5500 scanning electron microscope of the Center for Collective Use of the Krasnoyarsk Scientific Center.

Mössbauer spectra were measured on an MC-1104E5m spectrometer with the ⁵⁷Co(Cr) source at room temperature on powder samples with a thickness of 5–10 mg/cm² on the basis of the natural iron

* Corresponding author.

E-mail address: yar-man@bk.ru (R.N. Yaroslavtsev).<https://doi.org/10.1016/j.jmmm.2020.166979>

Received 15 October 2019; Received in revised form 13 January 2020; Accepted 6 May 2020

Available online 07 May 2020

0304-8853/ © 2020 Elsevier B.V. All rights reserved.

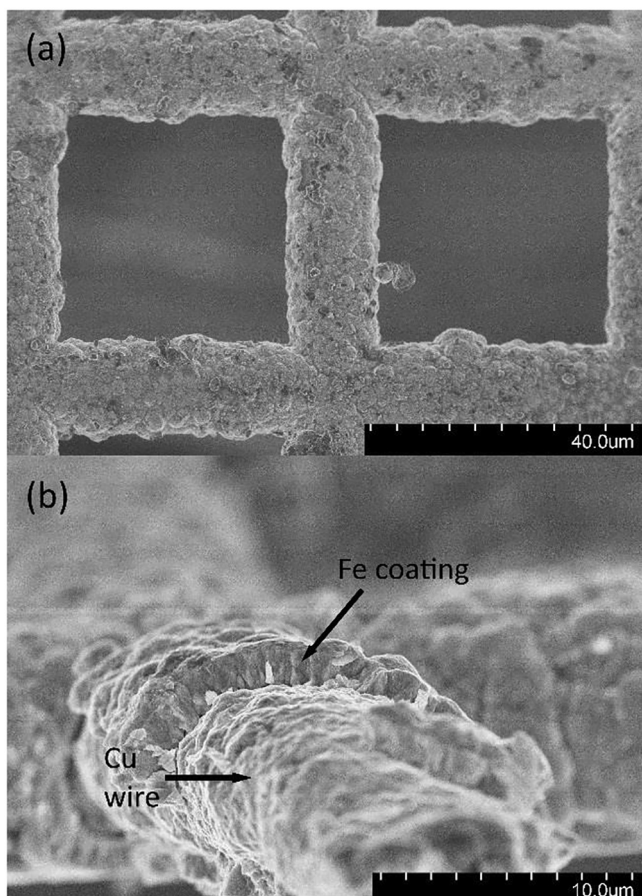


Fig. 1. SEM-images. $\times 1300$ (a) and $\times 5000$ (b).

content. Isomer chemical shifts are accounted in reference to α -Fe.

In-plane angular dependences (at 5° angular resolution) of ferromagnetic resonance (FMR) spectra measured with the X-band (9.7 GHz) spectrometer ELEXSYS E580 (Bruker, Germany).

3. Results and discussion

Figs. 1 and 2 show the results of microscopic studies of the magnetic metallic coating of Fe on a copper microgrid. The top view and cross-section of the sample are shown in Fig. 1. In Fig. 1(b), a textured

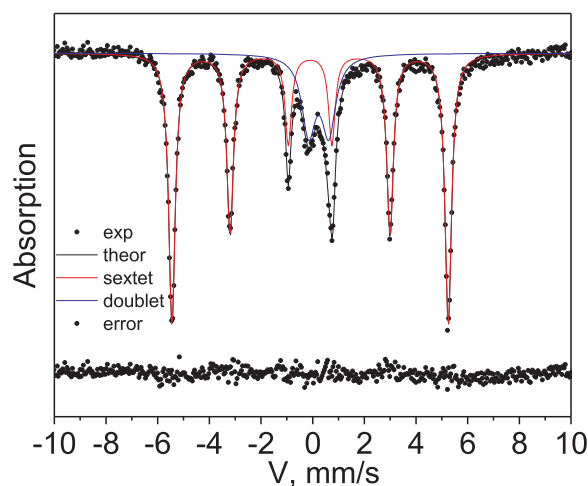


Fig. 3. Mössbauer spectrum of iron coating on a copper microgrid.

coating with a columnar radial structure is observed. Fig. 2a shows the image of the cross-section of the coating obtained using a transmission electron microscope, as well as the distribution of elements obtained by energy dispersive x-ray analysis. Elemental analysis (Fig. 2c, d, e) showed that the metal coating consists of iron. The presence of palladium is due to a thin sublayer on the surface of the wire. The diffraction pattern (Fig. 2b) confirms the presence of the α -Fe phase in the prepared coating.

The Mössbauer spectrum was obtained at room temperature (Fig. 3). The spectrum consists of a sextet and a doublet due to Fe^{3+} cations with octahedral coordination. The results of the interpretation are shown in Table 1. A doublet with a relative area of about 22% refers to an iron compound in a paramagnetic or superparamagnetic state (oxide, hydroxide or oxyhydroxide). The ferromagnetic contribution (sextet) with a relative area of 78% refers to the bcc-Fe phase.

Fig. 4 shows the microwave absorption spectra of the test sample. The magnetic field was applied parallel to the plane of the grid at different angles relative to one side of the grid. Fig. 5 shows the dependences of the resonance field and the FMR linewidth of the angle θ of rotation of the grid. The largest value of the resonance field and linewidth in the polar diagram corresponds to the direction of the axis along the side of the cell. Thus, the figure shows that the studied grid is characterized by two axes orthogonal to each other, oriented along with two tube systems. The width of the microwave absorption line, depending on the angle relative to the external field, varied in the range

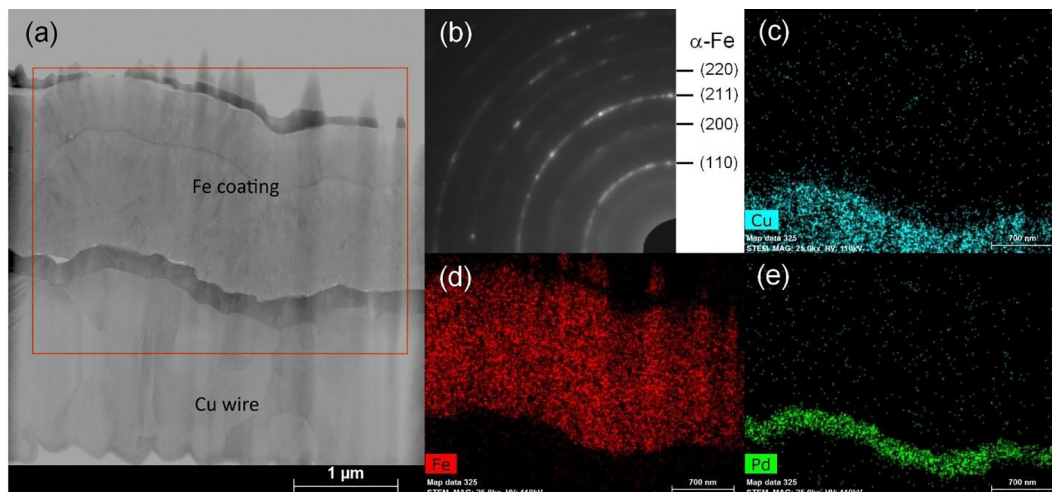


Fig. 2. TEM-image (a), microdiffraction pattern (b) and distribution of elements in the sample (c, d, e).

Table 1
Mössbauer parameters.

IS, mm/s	H, T	QS, mm/s	W, mm/s	A	Position
0.01	33.2	0	0.31	0.78	α -Fe
0.34	–	0.78	0.65	0.22	Fe^{3+} (6)

IS - isomeric shift; QS - quadrupole splitting;
W - absorption line width; H - hyperfine splitting field; A - fractional occupancy.

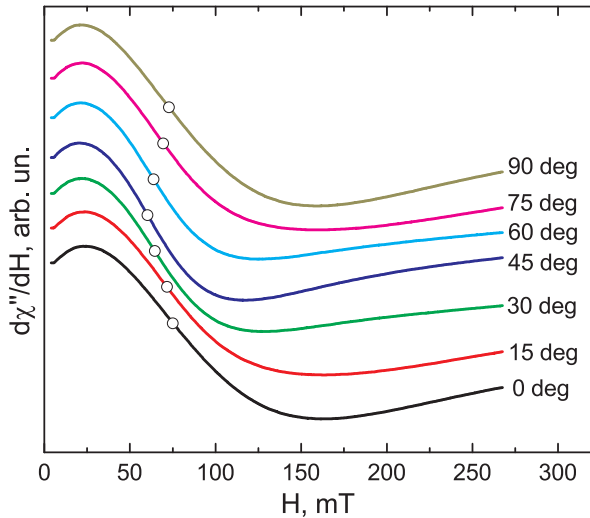


Fig. 4. FMR spectra of iron coating on a copper microgrid. Empty symbols indicate the resonance field.

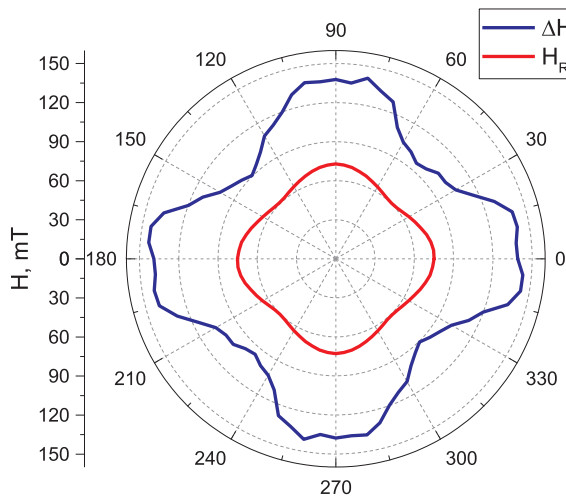


Fig. 5. Polar plot of resonance field and linewidth.

from 90 to 140 mT, which significantly exceeds the width of the FMR line in the films [18]. High values of the microwave absorption line width suggest the use of such materials for electromagnetic shielding.

The ferromagnetic resonance spectrum of the microgrid should consist of two signals related to two tube systems, which, when the grid is rotated, are shifted towards each other and merge into one at an angle of 45° relative to the field. However, this is not observed in these spectra. This is probably since the signal from the tube oriented along the field goes into negative fields due to the high magnetization of the iron coating.

The results of measuring the ferromagnetic resonance of a magnetic tube system can be described if the individual tube is considered as a

twisted thin film. The resonance field of the FMR of one tube oriented parallel to the field should coincide with the resonance field of a thin film also oriented parallel to the field. According to this model, when the field is oriented along the tube, the resonance field can be easily calculated by Kittel formula [19] and it will be 40 mT. According to the Kittel formula for polycrystal, the resonance field is determined by magnetization of sample and demagnetization factors that depend on the shape of the sample:

$$(\omega/\gamma)^2 = [H_0 + (N_x - N_z)M_0][H_0 + (N_y - N_z)M_0], \quad (1)$$

where γ – gyromagnetic ratio, ω – frequency, N_x , N_y , N_z – demagnetization factors of sample, H_0 – magnetic field, M_0 – magnetization.

In general, Kittel's formula is not suitable for samples in the form of a tube, because the tube is not an ellipsoid of revolution. However, if we consider the tube as a twisted film, then this formula can be used for orientation in parallel and perpendicular to the field. For the case of a film-shaped sample, demagnetizing factors are: $N_x = 0$, $N_y = 0$, $N_z = 1$.

The resonance from a tube oriented perpendicular to the field can be represented as the sum of the resonance curves of small planar sections covering the surface of the tube, etc. rotated by angles from 0 to 90° concerning the external field [20]. The resonance field of planar sections rotated at different angles concerning the field can be calculated using the Smith-Beljers formalism [21,22]. In this orientation, the resonance field is 44 mT. In this experiment, the resonance field of the observed peak varied in the range from 60 to 75 mT. This result may be because, in contrast to the model situation, where the thickness of the magnetic film is much less than the diameter of a cylindrical copper thread, the thickness of the test coating is comparable to this diameter.

Using an approach that considers the tube as the sum of flat sections, a ferromagnetic resonance curve can be modeled. Fig. 6 shows the FMR curve measured at an angle $\theta = 0^\circ$, as well as the fitting curve. The fitting curve is obtained by summing two resonance curves (from a tube oriented along the field and a tube oriented perpendicular to the field). The resonance curve for parallel orientation was a Lorentzian curve. The resonance curve for the perpendicular orientation was the sum of many Lorentzian curves from films rotated at different angles with respect to the field. The effective magnetization $M_{\text{eff}} = 1100$ kA/m and the uniaxial anisotropy field $H_a = 220$ mT were used as fitting parameters. M_{eff} differs from saturation magnetization (for bcc-Fe, the saturation magnetization is $M = 1700$ kA/m) by contributions due to

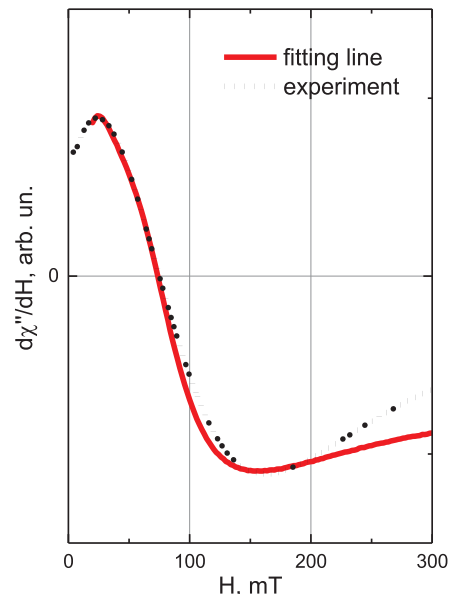


Fig. 6. FMR curve measured at an angle $\theta = 0^\circ$ and the fitting curve.

elastic stresses. The synthesis method we use leads to the formation of graphite inclusions in the magnetic coating. These inclusions are the source of local demagnetizing fields, which also lead to a decrease in the effective magnetization. Uniaxial radial anisotropy is a consequence of the texture formed in the coating (columnar structure) (see Fig. 1(b)).

4. Conclusion

Ferromagnetic iron coatings on the copper microgrid were prepared by electroless deposition. Angular dependence of the ferromagnetic resonance spectra revealed that the grid is characterized by two axes orthogonal to each other, oriented along with two tube systems. Modeling the lineshape of ferromagnetic resonance using an approach that considers the tube as a twisted thin film, allowed us to determine the effective magnetization and the field of uniaxial anisotropy.

CRedit authorship contribution statement

S.V. Stolyar: Supervision, Data curation, Writing - original draft, Conceptualization. **R.N. Yaroslavtsev:** Investigation, Data curation, Writing - original draft, Visualization. **L.A. Chekanova:** Investigation. **M.V. Rautskii:** Investigation. **O.A. Bayukov:** Investigation. **E.V. Cheremiskina:** Investigation. **I.V. Nemtsev:** Investigation. **M.N. Volochaev:** Investigation. **R.S. Iskhakov:** Supervision, Writing - review & editing.

Acknowledgments

This work was supported by Russian Foundation for Basic Research, Government of Krasnoyarsk Territory, Krasnoyarsk Region Science and Technology Support Fund to the research project No. 18-42-240006. We are grateful to the Center of collective use of FRC KSC SB RAS for the provided equipment.

References

- [1] S.S.P. Parkin, M. Hayashi, L. Thomas, Magnetic domain-wall racetrack memory, *Science* (80-) 320 (2008) 190–194, <https://doi.org/10.1126/science.1145799>.
- [2] A. Bordet, L.-M. Lacroix, P.-F. Fazzini, J. Carrey, K. Soulantica, B. Chaudret, Magnetically induced continuous CO₂ hydrogenation using composite iron carbide nanoparticles of exceptionally high heating power, *Angew. Chem. Int. Ed.* 55 (2016) 15894–15898, <https://doi.org/10.1002/anie.201609477>.
- [3] T. Uchiyama, K. Mohri, Y. Honkura, L.V. Panina, Recent advances of Pico-tesla resolution magneto-impedance sensor based on amorphous wire CMOS IC MI sensor, *IEEE Trans. Magn.* 48 (2012) 3833–3839, <https://doi.org/10.1109/TMAG.2012.2198627>.
- [4] J. Chen, L. Xu, W. Li, X. Gou, α -Fe₂O₃ nanotubes in gas sensor and lithium-ion battery applications, *Adv. Mater.* 17 (2005) 582–586, <https://doi.org/10.1002/adma.200401101>.
- [5] J. Alonso, H. Khurshid, V. Sankar, Z. Nemati, M.H. Phan, E. Garayo, J.A. García, H. Srikanth, FeCo nanowires with enhanced heating powers and controllable dimensions for magnetic hyperthermia, *J. Appl. Phys.* 117 (2015) 17D113, <https://doi.org/10.1063/1.4908300>.
- [6] B. Özkale, N. Shamsudhin, G. Chatzipirpiridis, M. Hoop, F. Gramm, X. Chen, X. Martí, J. Sort, E. Pellicer, S. Pané, Multisegmented FeCo/Cu nanowires: electrosynthesis, characterization, and magnetic control of biomolecule desorption, *ACS Appl. Mater. Interfaces* 7 (2015) 7389–7396, <https://doi.org/10.1021/acsami.5b01143>.
- [7] D. Lee, R.E. Cohen, M.F. Rubner, Heterostructured magnetic nanotubes †, *Langmuir* 23 (2007) 123–129, <https://doi.org/10.1021/la061292e>.
- [8] B.-I. Nam, J.-U. Kim, K.-H. Kim, RF power absorption enhancement of magnetic composites with conductive grid, *J. Magn.* 17 (2012) 129–132, <https://doi.org/10.4283/JMAG.2012.17.2.129>.
- [9] M. Darques, J. Spiegel, J. De la Torre Medina, I. Huynen, L. Piraux, Ferromagnetic nanowire-loaded membranes for microwave electronics, *J. Magn. Magn. Mater.* 321 (2009) 2055–2065, <https://doi.org/10.1016/j.jmmm.2008.03.060>.
- [10] L.-P. Carignan, A. Yelon, D. Menard, C. Caloz, Ferromagnetic nanowire metamaterials: theory and applications, *IEEE Trans. Microw. Theory Tech.* 59 (2011) 2568–2586, <https://doi.org/10.1109/TMTT.2011.2163202>.
- [11] Z.K. Wang, H.S. Lim, H.Y. Liu, S.C. Ng, M.H. Kuok, L.L. Tay, D.J. Lockwood, M.G. Cottam, K.L. Hobbs, P.R. Larson, J.C. Keay, G.D. Lian, M.B. Johnson, Spin waves in nickel nanorings of large aspect ratio, *Phys. Rev. Lett.* 94 (2005) 137208, <https://doi.org/10.1103/PhysRevLett.94.137208>.
- [12] H. Leblond, V. Veerakumar, Magnetostatic spin solitons in ferromagnetic nanotubes, *Phys. Rev. B* 70 (2004) 134413, <https://doi.org/10.1103/PhysRevB.70.134413>.
- [13] A. Janutka, K. Brzuszek, Domain-wall-assisted giant magnetoimpedance of thin-wall ferromagnetic nanotubes, *J. Magn. Magn. Mater.* 465 (2018) 437–449, <https://doi.org/10.1016/j.jmmm.2018.06.007>.
- [14] J. Sudagar, J. Lian, W. Sha, Electroless nickel, alloy, composite and nano coatings – a critical review, *J. Alloys Compd.* 571 (2013) 183–204, <https://doi.org/10.1016/j.jallcom.2013.03.107>.
- [15] A. Brenner, G.E. Riddell, Nickel plating on steel by chemical reduction, *J. Res. Natl. Bur. Stand.* 37 (1946) (1934) 31, <https://doi.org/10.6028/jres.037.019>.
- [16] E.R. Gasilova, G.N. Matveeva, G.P. Aleksandrova, B.G. Sukhov, B.A. Trofimov, Colloidal aggregates of Pd nanoparticles supported by larch arabinogalactan, *J. Phys. Chem. B* 117 (2013) 2134–2141, <https://doi.org/10.1021/jp3118242>.
- [17] S.V. Stolyar, S.V. Komogortsev, L.A. Chekanova, R.N. Yaroslavtsev, O.A. Bayukov, D.A. Velikanov, M.N. Volochaev, E.V. Cheremiskina, M.S. Bairmani, P.E. Eroshenko, R.S. Iskhakov, Magnetite nanocrystals with a high magnetic anisotropy constant due to the particle shape, *Tech. Phys. Lett.* 45 (2019) 878–881.
- [18] A.B. Vaganov, B. Heinrich, Magnetic resonance in epitaxial iron films, *JETP* 32 (1971) 399.
- [19] C. Kittel, On the theory of ferromagnetic resonance absorption, *Phys. Rev.* 73 (1948) 155–161, <https://doi.org/10.1103/PhysRev.73.155>.
- [20] L.A. Chekanova, E.A. Denisova, R.N. Yaroslavtsev, S.V. Komogortsev, D.A. Velikanov, A.M. Zhizhaev, R.S. Iskhakov, Micro grid frame of electroless deposited Co-P magnetic tubes, *Solid State Phenom.* 233–234 (2015) 64–67, <https://doi.org/10.4028/www.scientific.net/SSP.233-234.64>.
- [21] H. Suhl, Ferromagnetic resonance in nickel ferrite between one and two kilomegacycles, *Phys. Rev.* 97 (1955) 555–557, <https://doi.org/10.1103/PhysRev.97.555.2>.
- [22] J. Smit, H.G. Beljers, Ferromagnetic resonance absorption in BaFe₂O₁₉, a highly anisotropic crystal, *Philips Res. Rep.* 10 (1955) 113–130.